[CANCER RESEARCH 51, 5329-5338, October 1, 1991]

Folate-binding Protein Is a Marker for Ovarian Cancer

Ian G. Campbell, Tania A. Jones, William D. Foulkes, and John Trowsdale[1]

Imperial Cancer Research Fund, P.O. Box 123, Lincoln's Inn Fields, London WC2A 3PX, England

ABSTRACT

We describe the isolation of a complementary DNA (cDNA) sequence encoding the ovarian cancer-associated antigen recognized by monoclonal antibody MOv18 and its identification as a high-affinity folate-binding protein (FBP). Functional cDNA clones were isolated using mRNA from the ovarian carcinoma cell line SKOV3 and colon carcinoma cell line HT29, by transient expression in WOP cells and selection of expressing cells by adhesion to antibody-coated magnetic beads. The cDNAs differed in the lengths of 5'- and 3'-noncoding regions, but they encoded identical peptides. A database search clearly showed them to be adult high-affinity FBPs with amino acid sequences identical with those isolated from normal placenta and several carcinoma cell lines. Reactivity of cell lines with MOv18 was quantitatively consistent with the expression of FBP mRNA. Southern hybridizations show evidence of a family of related genes and/or pseudogenes and were mapped to chromosome 11q13.3-14.1 by fluorescent *in situ* hybridization using cosmid clones containing part of this region. Also identified were two *Pst*I polymorphisms of four and three alleles, respectively, and a two-allele *Msp*I polymorphism. The folate-binding protein locus was not amplified in any of the 16 carcinoma cell lines tested and in only 1 of 10 serous adenocarcinomas, indicating that overexpression of FBP in ovarian cancer cannot, in general, be due to gene amplification.

INTRODUCTION

Ovarian cancer accounts for more than half of the deaths due to gynecological malignancy with a 5-year survival rate of only 20–30% (1). The poor prognosis in ovarian cancer is generally due to the advanced stage of the disease at the time of diagnosis. There is clear evidence that detection at an earlier stage results in a better prognosis, and this has prompted the search for tumor-associated antigens which can be used as targets for MAbs[2] for both diagnostic and therapeutic purposes. One of the most useful MAbs to date is OC125 which recognizes approximately 80% of ovarian cancers and is used widely for diagnosis and for monitoring response to therapy (2). CA125, the antigen defined by OC125, is not truly specific to ovarian cancer because it can also be found in normal celomic derived epithelium and elevations of CA125 are also found in patients with other cancers and in those without malignant disease (3).

Recently, new MAbs have been developed in an attempt to achieve better specificities, but many still react with non-ovarian neoplastic tissue as well as normal tissue. The reason for this is that most MAbs directed against human cancer-associated antigens recognize epitopes consisting of carbohydrate or glycolipid and are associated with high M_r glycoproteins or mucins of cell membranes (4). These high M_r molecules are also expressed on normal tissue, and MAbs directed against epitopes on them often react with a diverse range of normal and tumor tissue (5). Miotti *et al.* (6) suggested that MAbs to these high molecular weight molecules predominate because they are highly immunogenic in mice. In an attempt to produce novel MAbs against other molecules, they used as immunogen a membrane preparation from a surgical specimen of an ovarian carcinoma which was completely negative with their other MAbs. One MAb produced in this way, MOv18, recognized epitopes on a glycoprotein of M_r 38,000–40,000 (CaMOv18) restricted to ovarian tumors. Initial investigation indicated that this antigen was expressed only in nonmucinous adenocarcinomas (72%) and adenomas (100%) and in a limited number of other carcinomas of the breast and lung but was completely absent on normal tissue. In a further investigation using an immunoperoxidase test, the sensitivity of MOv18 was confirmed with 82% of nonmucinous ovarian carcinomas positive, while normal ovary, uterus, and vagina were negative (7). However, normal fallopian tubes and adult renal proximal and distal tubules were shown to react with MOv18 as well as 64% of malignant uterine carcinomas, 2 of 2 benign hyperplasias of the uterus, and 2 of 3 renal carcinomas. Others have confirmed the sensitivity of MOv18 and extended studies to other cancers (8–10).

When monoclonal antibodies to proteins associated with tumors become available, it is desirable to clone and sequence nucleic acids encoding them. This information may provide insights into selective mechanisms involved in tumor growth and may also indicate a route for therapy or for the development of novel reagents for detection. In this paper we describe the cloning of CaMOv18 by transient expression in WOP cells and selection of expressing cells by adhesion to antibody-coated magnetic beads.

MATERIALS AND METHODS

Cell Culture. The cell lines used in these experiments are described in Table 1. Cells were grown at 37°C in 6% CO_2 in medium supplemented with 10% FCS, 100 units/ml penicillin, and 100 units/ml streptomycin. All cells were grown in Dulbecco's modified Eagle's medium with the following exceptions. TR175 and JA-1 were grown in Ham's F-12 medium (Gibco, Glasgow, Scotland), OVCA432 and OVCA433 were grown in modified Eagle's medium supplemented with nonessential amino acids, and PE/01 and PE/04 were grown in RPMI supplemented with 2.5 μg/ml insulin.

Monoclonal Antibodies. MAb MOv18 was kindly supplied by Dr. M. I. Colnaghi (Istituto Nazionale per lo Studio e la Cura dei Tumori, Milan, Italy). Affinity-purified sheep anti-mouse IgG-coated magnetic beads (Dyna-beads) were purchased from Dynal, Great Neck, NY. FITC IgG fraction rabbit anti-mouse IgG was purchased from Dako Corp.

cDNA Libraries. A cDNA library from colon carcinoma cell line HT29 in expression vector CDM8 (32) was kindly supplied by David Simmonds (Imperial Cancer Research Fund, Oxford, England). A cDNA library of approximately 2×10^6 recombinants was prepared from ovarian carcinoma line SKOV3 in the expression vector pKS1 using the *Bst*XI-cloning site. This vector was kindly supplied by George Stark (Imperial Cancer Research Fund, London, England) and contains CDM8 sequence 1535–4440 with pUC18 sequence 440–2501, essentially CDM8 with the *sup*F suppressor replaced with the ampicillin resistance gene of pUC8. The bacterial hosts for CDM8 and pKS1 were MC1061/P3 and DH5, respectively.

WOP Cell Transfection. Murine WOP 3027 cells are derivatives of mouse NIH3T3 cells (33) and support the replication of plasmids

Received 3/8/91; accepted 7/25/91.

The costs of publication of this article were defrayed in part by the payment of page charges. This article must therefore be hereby marked *advertisement* in accordance with 18 U.S.C. Section 1734 solely to indicate this fact.

[1] To whom requests for reprints should be addressed.

[2] The abbreviations used are: MAb, monoclonal antibody; FITC, fluorescein isothiocyanate; PBS, phosphate-buffered saline; FACS, fluorescence-activated cell sorter; FCS, fetal calf serum; SDS, sodium dodecyl sulfate; FBP, folate-binding protein; cDNA, complementary DNA; poly(A)$^+$ RNA, polyadenylated RNA; SSC, standard sodium citrate; GPI, glycosyl-phosphatidylinositol.

Table 1 *Expression of CaMOv18 among cell lines*

Cell line	Source	FACS[a]	FBP mRNA[b]	Ref.
SKOV3	Ovarian carcinoma	10	++	11
OVCA432	Ovarian carcinoma	24	+++	2
OVCA433	Ovarian carcinoma	5	++	2
PE/O1	Ovarian carcinoma	0	−	12
PE/O4	Ovarian carcinoma	9	++	12
JA-1	Ovarian carcinoma	0	−	13
TR175	Ovarian carcinoma	0	−	13
JAMA	Ovarian carcinoma	0	−	[c]
SW620	Colon adenocarcinoma	30	+++	14
HT29	Colon adenocarcinoma	1	++	15
SW1222	Colon adenocarcinoma	0	−	14
LS-174T	Colon adenocarcinoma	0	−	16
LoVo	Colon adenocarcinoma	15	+++	17
SW1417	Colon adenocarcinoma	nt	−	[d]
DLD-1	Colon adenocarcinoma	nt	++	18
HCT-116	Colon adenocarcinoma	nt	++	19
CC20	Colon adenocarcinoma	nt	−	20
MCF-7	Breast adenocarcinoma	3	nt	21
SkBR3	Breast metastatic pleural effusion	0	nt	22
NB100	Neuroblastoma	0	nt	[e]
EJ	Bladder carcinoma	0	nt	23
HT1080	Fibrosarcoma	0	nt	24
HeLa S3	Epithelioid carcinoma of cervix	60	++++	25
HEp-2	Epidermoid carcinoma of larynx	18	+++	25
MOLT-4	Lymphoblastic leukemia	0	nt	26
DX3	Melanoma	nt	+	27
Mann	B-cell	nt	−	28
MRC5	Normal fetal lung	nt	−	29
PAF	Fibroblast	nt	−	30
SV80	Fibroblast	nt	−	31

[a] Relative fluorescence with MOv18 measured in arbitrary units. nt, not tested.
[b] Summary of Northern hybridization with cHTMOv18 probe shown in Fig. 6. Indication of intensity of signal above background (in folds): −, no signal; +, 2–5; ++, 5–10; +++, 10–100; ++++, >100.
[c] Obtained from Dr. S. Malik, Imperial Cancer Research Fund, London, England.
[d] American Type Culture Collection, ATCC 238.
[e] Obtained from Dr. A. Evans, Children's Hospital, Philadelphia, PA.

containing the polyoma virus origin (32). Plasmid DNA was introduced into WOP cells by electroporation based on the method described by Chu *et al.* (34). The WOP cells, passaged 16–20 h previously, were harvested at 50–75% confluence by treatment with trypsin/EDTA and washed twice with HeBs buffer [20 mM 4-(2-hydroxyethyl)-1-piperazineethanesulfonic acid, pH 7.05-137 mM NaCl-5 mM KCl-0.7 mM Na_2HPO_4-6 mM dextrose]. The cells were resuspended at 2×10^7/ml in HeBs containing 200 μg/ml sheared herring sperm DNA as carrier and 50 μg/ml of plasmid cDNA library. Aliquots of 500 μl were transferred to 0.4-cm electroporation curvettes (Bio-Rad 165-2088) and pulsed at 300 V with a capacitance of 250 μF. The time constant was between 4.5 and 5.5 ms. The cells were left at room temperature for 5 min and then washed three times in medium before seeding. Cells were incubated for 48–72 h to allow expression.

Recovery of cDNA Clones by Binding to Magnetic Beads. Detachment and antibody treatment of transfected WOP cells and recovery of plasmid DNA were carried out as described by Aruffo and Seed (35) except that magnetic beads rather than antibody-coated dishes were used for recovery of CaMOv18-expressing cells. Briefly, the antibody-treated cells were resuspended in 1–2 ml PBS-0.5 mM EDTA-0.02% sodium azide-5% FCS. Affinity-purified sheep anti-mouse IgG-coated magnetic beads (50–100 μl) were added, and the cells were incubated on ice for 1 h with periodic gentle shaking. Cells coated with magnetic beads were recovered by 4 washes in PBS-EDTA-FCS using a magnetic particle concentrator according to the recommendations of the manufacturer (Dynal). Two ml 10 mM EDTA-0.6% SDS was added to the recovered cells, and after 5 min 0.5 ml 5 M NaCl was added and incubation continued for 4 h on ice. The cell debris was then pelleted and the supernatant extracted once with phenol chloroform. Glycogen was added to a concentration of 20 μg/ml and the DNA recovered by ethanol precipitation. The resulting DNA was resuspended in 20 μl water and 5 μl was transformed by electroporation into either MC1061/p3 or DH5. The resulting colonies were pooled and amplified in liquid culture, and plasmid DNA was prepared (36). The resulting plasmid DNA was purified by CsCl gradient centrifugation and used in the next cycle of transfection. After the third round of transfection, individual colonies were picked, and plasmid DNA from each of these was prepared and used to transfect WOP cells.

RNA and DNA Blot Analyses. Poly(A)$^+$ RNA was isolated from the cells lines using a commercial kit (Fast Track, Invitrogen) and 0.5 μg poly(A)$^+$ was loaded on a 1% agarose-2.2 M formaldehyde gel in 1× 4-morpholinepropanesulfonic acid buffer (37). The RNA was transferred in 0.05 M NaOH to Hybond N$^+$ (Amersham). DNA was electrophoresed on 0.7% agarose gels and was transferred to Hybond N$^+$ with 0.4 M NaOH. Hybridization was carried out in 5× SSC-0.2% SDS-10% dextran sulfate with random primed [^{32}P]dCTP-labeled DNA probes. The membranes were washed under high stringency conditions (0.1× SSC-0.1% SDS at 65°C; 1× SSC = 0.15 M NaCl-0.015 M sodium citrate).

Somatic Cell Hybrid Mapping. The somatic cell hybrid lines from which DNA was derived have been described (Table 2). The DNA from parental and hybrid cells was digested with *Bam*HI and analyzed in Southern blots.

***In Situ* Hybridization.** Spreads of human metaphase chromosomes from peripheral blood lymphocytes were obtained by standard procedures. Cosmid DNA was biotinylated using the Bionick kit (BRL), purified through a Sephadex G-50 column, and then precipitated with salmon sperm DNA and *Escherichia coli* tRNA. *In situ* hybridization and detection were performed using a modification of the technique described by Pinkel *et al.* (46). Labeled probe DNA (80 ng) was combined with 2.5 μg of unlabeled genomic DNA (in order to block nonspecific sequences) and 20 ng of labeled centromere probe.

Slides were mounted with Citifluor containing 0.5 μg/ml propidium iodide. Color photographs were taken on a Fujicolor HG400 print film using a Ziess photomicroscope III with Ziess filter set 9. Only chromosomes with paired signals (a signal on each chromatid of the same chromosome) were scored. The band localization of the probe was determined by calculating the fractional length relative to the distance from 11cen to 11qter (47). The overall mean ratio (and SEM) was calculated. A mean value ± 2 SD provides a 95% confidence limit. This measurement was then compared with standard karyotypes (48) to determine the corresponding band localization.

FACS and Fluorescence Microscopy. Cells (1×10^6) were harvested, washed with cold PBS containing 5% FCS, and then resuspended in 50 μl MOv18 diluted in PBS-5% FCS to 0.5 μg/ml. After 30 min on ice, the cells were washed twice in PBS-5% FCS, resuspended in 50 μl of 100 μg/ml FITC-conjugated IgG fraction rabbit anti-mouse IgG, and incubated an additional 30 min on ice. The cells were washed twice, resuspended in cold PBS, and analyzed on the FACScan (Becton Dickinson and Co.) or observed by fluorescence microscopy. A negative control of cells stained with fluorescenated antibody only was included. An estimate of the relative fluorescence intensity in arbitrary units was made by subtracting the mean fluorescence of the cells treated only with FITC from the mean fluorescence of the MOv18 plus FITC-treated cells.

RESULTS

Isolation of a cDNA Encoding CaMOv18 Antigenic Determinant. The HT29 colon and SKOV3 ovarian carcinoma line cDNA libraries were introduced separately into WOP cells, and 48–72 h later CaMOv18 positive transfectants were selected with MOv18 antibody and sheep anti-mouse IgG antibody-coated magnetic beads. The CaMOv18-enriched plasmid prepared from these cells was then transformed into bacteria, and the resulting colonies were pooled and used to prepare plasmid DNA for the next round of WOP cell transfection. This cycle was repeated until the end of the third round when plasmid DNA was prepared from 10 individual bacterial transformants from each library and transfected separately into WOP cells. Three of the 10 HT29 clones and 5 of the SKOV3 clones showed surface expression of CaMOv18 as detected by indirect

Table 2 *FBP chromosome assignment with rodent/human somatic hybrids*

	Ref.	Human chromosomes																						FBP locus[a]
		1	2	3	4	5	6	7	8	9	10	11	12	13	14	15	16	17	18	19	20	21	22	X	Y	
CL21E	38							+[b]																+		
DUR4.3	39			+		+					+	+	+	+	+	+		+	+		+	+	+	+		+
SIF4A31	40			+	+	+	+								+		+							+		
CTP34B4	41	+	+	+		+	+	+	+				+		+		+	+	+					+		
FIR 5	42					+		+					+		+				+					+		
B2	43											+[c]												+[c]		+
IB5	44											+[d]														+
M11X	45											+[e]												+[e]		+

[a] Presence of the FBP locus assessed by the presence of 22-, 7.8-, 6.4-, and 5.0-kilobase *Bam*HI bands.
[b] +, presence of a particular chromosome. Origin of the hybrids is described in the references listed in column 2.
[c] 11p13-11qter + Xpter-Xq11.
[d] 11pter-11q23.
[e] 11pter-11q24 + Xq22-qter.

immunofluorescence. Digestion of the resulting clones with *Xho*I and agarose gel electrophoresis showed inserts of 0.9 kilobases in all the HT29 clones and a 1.3-kilobase insert in all the SKOV3 clones.

cDNA Sequence Analysis. The CaMOv18 cDNAs from HT29 and SKOV3 were sequenced using a chain-termination protocol with supercoiled DNA templates. The cDNA derived from SKOV3, cSKMOv18, was 1325 base pairs and contained a 771-base pair open reading frame flanked by 5′- and 3′-noncoding sequences of 430 and 124 base pairs, respectively (Fig. 1). The 3′-noncoding region contained a polyadenylation signal (AATAAA) at 879 but did not contain a polyadenylate tail. The sequence derived from HT29, cHTMOv18, consisted of 936 base pairs. Compared with cSKMOv18, the sequence of cHTMOv18 begins at nucleotide −11 and contains an additional 31 base pairs of 3′-noncoding sequence as indicated in Fig. 1. The sequence was identical with cSKMOv18 apart from a single cytosine to thymine substitution in the open reading frame at position +588 and an adenine to guanine substitution at +799 in the 3′-untranslated region (Fig. 1). The deduced amino acid sequences for both cDNA were identical.

Similarity of CaMOv18 with Folate-binding Proteins. A database search revealed strong sequence identity between CaMOv18 and a human high-affinity folate-binding protein. The cDNA nucleotide sequences have been reported for two classes of folate-binding proteins (49), a putative adult form, isolated from epidermoid carcinoma (KB) cells (50), colon carcinoma cells Caco-2 (51), and placenta (52), and a putative fetal form also isolated from placenta (49). The nucleotide sequence comparison for cSKMOv18 with sequence from the adult FBPs isolated from KB cells (50) and Caco-2 cells (51) clearly shows it to be of the adult form. The sequences were identical downstream from nucleotide −10, apart from differing lengths of the 3′-noncoding regions and two nucleotide substitutions, a cytosine to thymine at position +588 in cHTMOv18 and a guanine to adenine at position +799 in cSKMOv18 (Fig. 1).

Differences in the 5′-noncoding region were evident between cSKMOv18 and the Caco-2 cell FBP and the KB cell FBP and appeared to be products of alternate RNA splicing at the junction of nucleotides −10 and −11 and between nucleotides −76 and −77 as illustrated in Fig. 2. All the sequences were homologous up to and including nucleotide −10. However, 5′ from this position the cSKMOv18 and Caco-2 sequences contained 66 base pairs of sequence not present in the KB cell FBP cDNA. At the end of this stretch of homology, at position −76, the cSKMOv18 and Caco-2 sequences diverged, and no further homology was evident between them. In contrast, homology with the KB cell FBP sequence which was interrupted at the first proposed splice junction (position −11 on the KB cell FBP) continued to the end of the sequence.

Another adult FBP sequence has been reported (52) isolated from KB cells. The sequence of this clone had several nucleotide substitutions and one single nucleotide deletion with respect to cSKMOv18 and the other published FBP sequences. Two cytosine to thymine substitutions at positions +586 and +588 resulted in a serine instead of a threonine at residue 161. In addition, a deletion of a cytosine at nucleotide +748 created an in-frame stop codon resulting in a predicted peptide which terminated at Ala-249 which was 8 residues shorter than that reported here. The reason for this discrepancy is unclear.

Southern Analysis. Southern blots were carried out to determine the complexity of the FBP sequences at the genomic level. *Eco*RI and *Bam*HI digests of SKOV3 and normal human DNA were hybridized with the cHTMOv18 cDNA (Fig. 3). Four major bands were visible with *Bam*HI (22.0, 7.8, 6.4, and 5.0 kilobases) as well as 6 other bands of lesser intensity (26.0, 14.7, 11.6, 3.9, 3.8, and 1.1 kilobases). *Eco*RI digests showed two major bands (20.0 and 7.9 kilobases) and 6 bands of lesser intensity (9.6, 8.8, 7.3, 5.8, 4.0, and 1.9 kilobases). The large number of bands visible in Southern blots suggests that the FBP family may contain more than the two members so far described and/or the existence of pseudogenes.

Screening for DNA Polymorphism. To identify restriction fragment length polymorphisms, DNA from 17–27 unrelated individuals were digested with a variety of enzymes and probed with cHTMOv18. No polymorphisms were detected with *Bam*HI, *Eco*RI, *Hind*III, and *Pvu*II.

Two *Pst*I polymorphisms were detected among 27 unrelated individuals. The first was a four-allele polymorphism with variable bands at 7.5 (allele A1), 6.8 (allele A2), 6.3 (allele A3), and 5.9 kilobases (allele A4) with frequencies of 0.04, 0.42, 0.5, and 0.04, respectively. The second was a three-allele polymorphism with variable bands at 4.2 (allele B1), 3.9 (allele B2), and 3.8 kilobases (allele B3) with frequencies of 0.61, 0.37, and 0.02, respectively. Numerous constant bands were also detected with this enzyme. An example blot is shown in Fig. 4*A*.

*Msp*I detected a two-allele polymorphism with fragment sizes of 4.5 (allele A1) or 3.2 kilobases (allele A2) as well as several constant bands (Fig. 4*B*). In some blots an additional band of 2.3 kilobases was observed but this was thought to be due to incomplete digestion. Among 22 unrelated individuals the allelic frequencies of A1 and A2 were 0.07 and 0.93, respectively. Mendelian codominant inheritance of the *Pst*I and *Msp*I alleles was demonstrated in one three-generation family and one two-generation family.

Somatic Hybrid Mapping of Folate-binding Gene. In order to map the FBP gene(s) Southern blots of *Bam*HI-digested DNAs

```
-430                                                                    -351
GGAAAGGATTTTCTCAGCCCCCATCTCCAGCACTGTGTGTTGGCCGCACCCATGAGAGCCTCAGCACTCTGAAGGTGCAG
                                                                        -271
GGGGCAAAGGCCAAAAGAGCTCTGGCCTGAACTTGGGTGGTCCCTACTGTGTGACTTGGGGCATGGCCTCATCTGTGCTG
                                                                        -191
AAATGATTCCACAAAGATTAAACTGGCTATCATTTGTTGATTTCCCCCTTCTTACATTTAATCCTTGCAGGAGAAAGCTA
                                                                        -111
AGCCTCAAGATAGTTTGCTTCTCTTTCCCCCAAGGCCAAGGAGAAGGTGGAGTGAGGGCTGGGGTCGGGACAGGTTGAAC
                                                                         -31
GGGAACCCTGTGCTCTAACAGTTAGGGCCCGCCGAGGAACTGAACCCAAAGGATCACCTGGTATTCCCTGAGAGTACAGA
                                        1                                 36
TTTCTCCGGCGTGGCCCTCAAGGGACAGAC   ATG GCT CAG CGG ATG ACA ACA CAG CTG CTG CTC CTT
                                 MET Ala Gln Arg MET Thr Thr Gln Leu Leu Leu Leu
                                 1                                        96
 CTA GTG TGG GTG GCT GTA GTA GGG GAG GCT CAG ACA AGG ATT GCA TGG GCC AGG ACT GAG
 Leu Val Trp Val Ala Val Val Gly Glu Ala Gln Thr Arg Ile Ala Trp Ala Arg Thr Glu
 13                                                                      156
 CTT CTC AAT GTC TGC ATG AAC GCC AAG CAC CAC AAG GAA AAG CCA GGC CCC GAG GAC AAG
 Leu Leu Asn Val Cys MET Asn Ala Lys His His Lys Glu Lys Pro Gly Pro Glu Asp Lys
 33                                                                      216
 TTG CAT GAG CAG TGT CGA CCC TGG AGG AAG AAT GCC TGC TGT TCT ACC AAC ACC AGC CAG
 Leu His Glu Gln Cys Arg Pro Trp Arg Lys Asn Ala Cys Cys Ser Thr Asn Thr Ser Gln
 53                                                                      276
 GAA GCC CAT AAG GAT GTT TCC TAC CTA TAT AGA TTC AAC TGG AAC CAC TGT GGA GAG ATG
 Glu Ala His Lys Asp Val Ser Tyr Leu Tyr Arg Phe Asn Trp Asn His Cys Gly Glu MET
 73                                                                      336
 GCA CCT GCC TGC AAA CGG CAT TTC ATC CAG GAC ACC TGC CTC TAC GAG TGC TCC CCC AAC
 Ala Pro Ala Cys Lys Arg His Phe Ile Gln Asp Thr Cys Leu Tyr Glu Cys Ser Pro Asn
 93                                                                      396
 TTG GGG CCC TGG ATC CAG CAG GTG GAT CAG AGC TGG CGC AAA GAG CGG GTA CTG AAC GTG
 Leu Gly Pro Trp Ile Gln Gln Val Asp Gln Ser Trp Arg Lys Glu Arg Val Leu Asn Val
 113                                                                     456
 CCC CTG TGC AAA GAG GAC TGT GAG CAA TGG TGG GAA GAT TGT CGC ACC TCC TAC ACC TGC
 Pro Leu Cys Lys Glu Asp Cys Glu Gln Trp Trp Glu Asp Cys Arg Thr Ser Tyr Thr Cys
 133                                                                     516
 AAG AGC AAC TGG CAC AAG GGC TGG AAC TGG ACT TCA GGG TTT AAC AAG TGC GCA GTG GGA
 Lys Ser Asn Trp His Lys Gly Trp Asn Trp Thr Ser Gly Phe Asn Lys Cys Ala Val Gly
 153                                                                     576
 GCT GCC TGC CAA CCT TTC CAT TTC TAC TTC CCC ACA CCC ACT GTT CTG TGC AAT GAA ATC
 Ala Ala Cys Gln Pro Phe His Phe Tyr Phe Pro Thr Pro Thr Val Leu Cys Asn Glu Ile
 173                T                                                    636
 TGG ACT CAC TCC TAC AAG GTC AGC AAC TAC AGC CGA GGG AGT GGC CGC TGC ATC CAG ATG
 Trp Thr His Ser Tyr Lys Val Ser Asn Tyr Ser Arg Gly Ser Gly Arg Cys Ile Gln MET
 193                                                                     696
 TGG TTC GAC CCA GCC CAG GGC AAC CCC AAT GAG GAG GTG GCG AGG TTC TAT GCT GCA GCC
 Trp Phe Asp Pro Ala Gln Gly Asn Pro Asn Glu Glu Val Ala Arg Phe Tyr Ala Ala Ala
 213                                                                     756
 ATG AGT GGG GCT GGG CCC TGG GCA GCC TGG CCT TTC CTG CTT AGC CTG GCC CTA ATG CTG
 MET Ser Gly Ala Gly Pro Trp Ala Ala Trp Pro Phe Leu Leu Ser Leu Ala Leu MET Leu
 233                771                               G                   829
 CTG TGG CTG CTC AGC TGA CCTCCTTTTACCTTCTGATACCTGAAAATCCCTGCCCTGTTCAGCCCCACAGCTC
 Leu Trp Leu Leu Ser End                           G
 253                                                          895
 CCAACTATTTGGTTCCTGCTCCATGGTCGGGCCTCTGACAGCCACTTTGAATAAACCAGACACCGCacatgtgtcttgaga

 attatttggaaaaaaa
```

Fig. 1. Complete nucleotide sequence of the SKOV3 folate-binding protein cDNA clone, cSKMOv18, and its predicted amino acid sequence. Polyadenylation signal (AATAAA) is underlined. Nucleotide positions based on the AUG start codon are numbered above the sequence and amino acid positions below. *Arrows*, putative RNA splice sites at nucleotides −10 and −76 (see also Fig. 2). The lowercase sequences in the 3′-noncoding region are present in cHTMOv18 but not cSKMOv18. Nucleotides indicated above the main sequence indicate substitutions found in cHTMOv18 and below substitutions in the Caco-2 cell (51) and KB cell (50) FBP sequences.

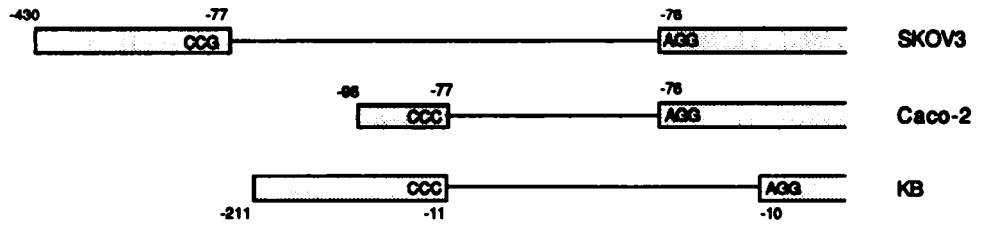

Fig. 2. Schematic presentation (not to scale) of the proposed alternative RNA splicing in FBP transcripts based on sequences from SKOV3 (this report), Caco-2 (51), and KB (50). *Shaded boxes*, cloned cDNA sequences; *horizontal lines*, proposed intron regions. Within the shaded boxes homologous sequences are aligned. Numbering is based on the AUG start codon.

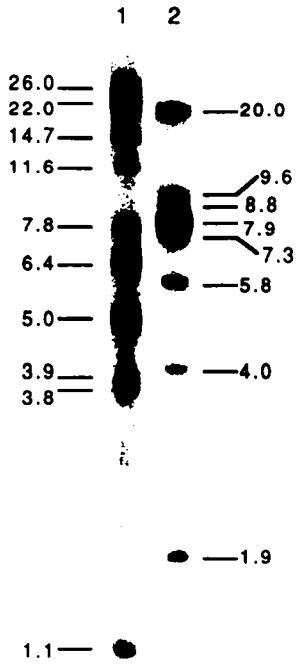

Fig. 3. Hybridization of the cHTMOv18 probe with normal human DNA digested with *Bam*HI (*lane 1*) and *Eco*RI (*lane 2*) washed under stringent conditions (0.1× SSC, 65°C). *Ordinates*, sizes of fragments in kilobases. These were calculated from *Hind*III-digested λ phage fragments run alongside.

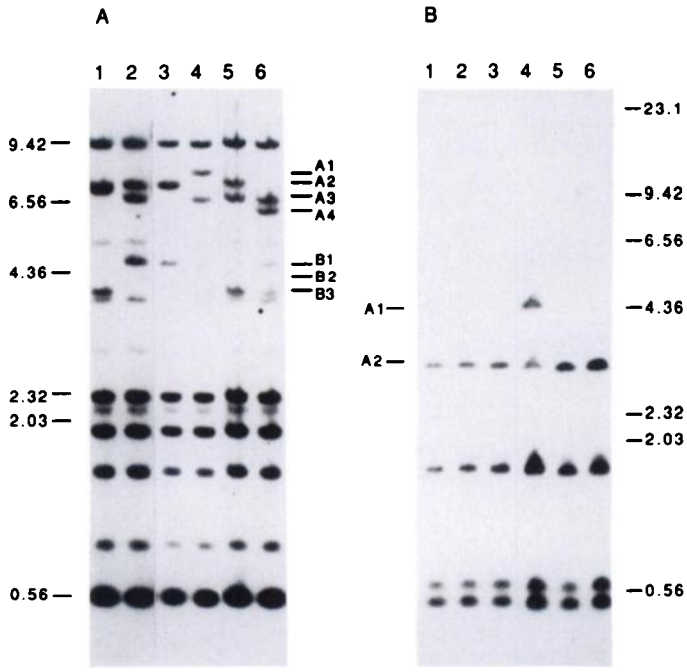

Fig. 4. Southern blot of human genomic DNA from 6 unrelated individuals showing *Pst*I (*A*) and *Msp*I (*B*) restriction fragment length polymorphisms detected by the cHTMOV18 probe and washed under stringent conditions (0.1× SSC, 65°C). *Ordinates* (*A, left; B, right*), sizes in kilobases of *Hind*III-digested λ phage molecular weight markers. *Ordinates*, fragments corresponding to the *Pst*I alleles (*A, right*) and to *Msp*I alleles (*B, left*). The B2 allele is not present in any of these individuals but when present migrates to this position.

from 6 human/rodent somatic cell hybrids containing a variety of human chromosomes were hybridized with the cHTMOv18 probe (Fig. 5*A*, Table 2). Four intense bands of 22.0, 7.8, 6.4, and 5.0 kilobases were seen with human DNA clearly distinguishable from the 4 faint bands in rat DNA and from mouse DNA, which showed one intense band at 4.0 kilobases and three faint bands at 6.0, 4.5, and 2.5 kilobases. DUR4.3 was the only hybrid showing human FBP bands and from this limited panel were localized to chromosomes 10, 11, 12, 13, 20, 21, or 22. Hybridization of a second panel of hybrids containing single human chromosomes localized the FPB bands to chromosome 11 (not shown). To confirm this, three hybrids containing segments of chromosome 11 were analyzed (Fig. 5*B*). Apart from one weakly hybridizing *Bam*HI band of 14.7 kilobases, all the fragments visible in the normal human control were present in each of the chromosome 11 hybrids. The only shared region between these hybrids is 11p13–11q23.

Isolation of Genomic DNA FBP Clones and *in Situ* Hybridization. In order to locate the FBP gene(s) precisely by fluorescent *in situ* hybridization, genomic clones containing part of this region were isolated. A cosmid genomic library derived from HPB-ALL cell line in the vector COS202 was screened using the cHTMOv18 probe. Seven positives were identified and restriction analysis showed they fell into classes represented by G4.1 (2 clones), G2.2 (1 clone), and G53.3 (4 clones). Hybridization of *Bam*HI digests of these with cHTMOv18 showed all contained a 6.4-kilobase fragment. In addition G4.1 contained the 22.0- and 3.8-kilobase *Bam*HI bands, while G53.3 contained the 7.8- and 3.8-kilobase bands. The latter clone showed the strongest hybridization with cHTMOv18 and was chosen for use in the *in situ* hybridization. Chromosome 11 was identified by hybridization with centromere probe D11Z1 (53). The positions of paired signals along chromosome arm 11q were measured on both chromatids of 14 copies of chromosome 11 from 6 metaphases. Fig. 6 shows an example of a metaphase cell hybridized under these conditions. Analysis showed a mean fractional length relative to the distance from 11cen to 11qter of 0.3024 with ± SD confidence limits of 0.2417–0.3631, corresponding to a location of 11q13.3–q14.1. No signals at other locations were observed.

Expression of FBP in Cancer Cell Lines. To confirm that a FBP was indeed the antigen to which MOv18 was reactive and to assess how widespread was its expression, various cell lines were examined by FACS using MOv18 (Table 1) and by Northern blot analysis using the cHTMOv18 cDNA as probe (Fig.

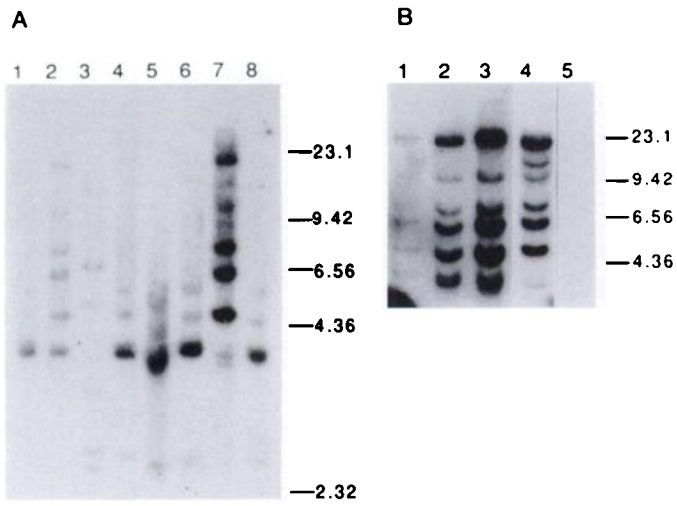

Fig. 5. Mapping of FBP to a human chromosome using human/rodent somatic hybrids digested with *Bam*HI and probed with cHTMOv18. *A: track 1*, CL.21E; *track 2*, DUR4.3; *track 3*, SIF4A31; *track 4*, CTP34B4; *track 5*, FIR 5; *track 6*, FIR 5; *track 7*, human DNA; *track 8*, mouse DNA. *B: track 1*, B2; *track 2*, IB5; *track 3*, M11X; *track 4*, human DNA; *track 5*, mouse DNA. *Ordinates*, sizes in kilobases of *Hind*III-digested λ phage molecular weight markers.

Fig. 6. *In situ* hybridization of cosmid G53.3 and chromosome 11 centromere probe D11Z1 with metaphase chromosomes of a normal male. *Arrows*, signals localized over 11q13.3–14.1.

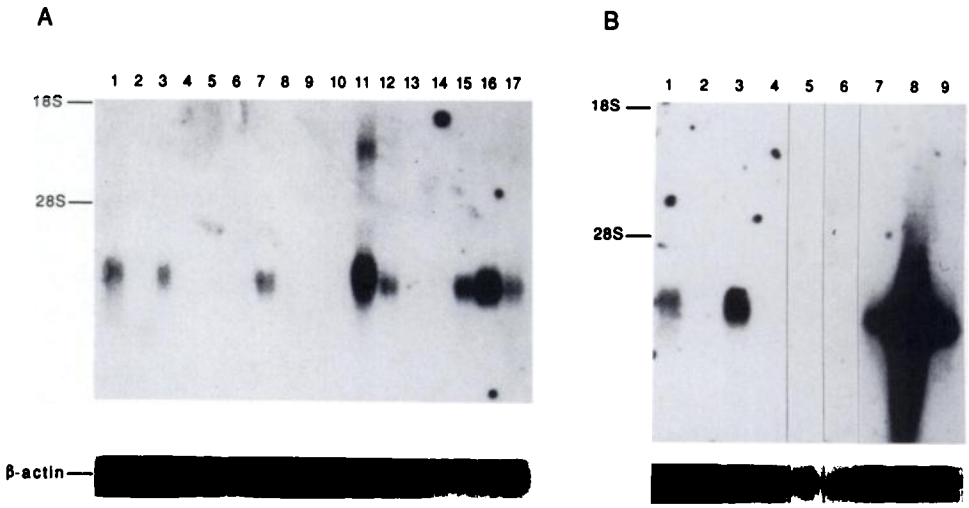

Fig. 7. Northern hybridization analysis of cell lines with cHTMOv18 probe. Poly(A)$^+$ RNA (5 μg) or total RNA (10 μg) was loaded onto 1% agarose-formaldehyde gels and electrophoresed at 25 V for 20 h. The gel was blotted onto Hybond N$^+$, probed with cHTMOv18 (*top*) or β-actin (*bottom*) as a loading control, and washed under stringent conditions (0.1× SSC, 65°C). *A: track 1*, SKOV3; *track 2*, PE/01; *track 3*, DX3; *track 4*, SV80; *track 5*, PAF; *track 6*, MRC5; *track 7*, HCT-116; *track 8*, MANN; *track 9*, CC20; *track 10*, SW1222; *track 11*, SW620; *track 12*, DLD-1; *track 13*, LS174T; *track 14*, SW1417; *track 15*, HT29; *track 16*, OVCA432; *track 17*, OVCA433. *B: track 1*, SKOV3; *track 2*, PE/01; *track 3*, PE/04; *track 4*, JAMA-2; *track 5*, TR175; *track 6*, JA-1; *track 7*, LoVo; *track 8*, HeLa; *track 9*, HEp2.

7). The intensity of mRNA signals above background were quantitated by laser densitometry and the data summarized in Table 1. Reactivity with MOv18 correlated quantitatively with the expression of FBP mRNA in all cases except HT29. In this case the mRNA signal obtained with the probe was greater than expected on the basis of the weak signal observed by FACS. A discrepancy in the binding of MOv18 and MOv19 to HT29 was observed by Miotti *et al.* (6). Even though both Mabs were shown to identify the same molecule, they reported that MOv19 reacted strongly to HT29, while MOv18 was unreactive by immunofluorescence (although weakly positive by radioimmune assay). Cloning of this antigen from HT29 has revealed only one species of FBP which when expressed in WOP cells is recognized by MOv18, suggesting that in HT29 posttranslational modification of the FBP results in the loss of the epitope recognized by MOv18 but not that of MOv19.

Only four of the eight ovarian lines expressed FBP at detectable levels, which is low considering the high frequency reported *in vivo*. Interestingly, PE/01 expressed no FBP as assessed by both FACS and Northern blotting, while PE/04, which was derived from the same patient, expressed moderate levels. Among the colon carcinoma lines FBP expression was similar with five of the nine lines showing FBP expression either by FACS and/or Northern blotting. The 13 lines which expressed FBP displayed great variability in relative levels from the weak mRNA signal shown by the melanoma cell line DX3 to HeLa with a signal 100-fold greater than SKOV3 and >1000-fold above background.

Copy Number FBP Genes in Cell Lines and Ovarian Tumors. To determine whether the wide variation in levels of FBP expression among the cell lines was due to differences in DNA levels or rearrangements, genomic DNA from the cell lines was digested with *Bam*HI and subjected to Southern analysis using the cHTMOv18 cDNA as probe (data not shown). The autoradiographs obtained were quantitated by laser densitometry and differences in DNA loading were corrected for by including chromosome 6 and/or 21 probes in the same hybridization. No amplification of the FBP locus was evident in any cell line. However, in HeLa and PE/01, differences in specific bands were observed. In HeLa cells, which express extremely high levels of FBP, one copy of the 7.8-kilobase *Bam*HI was absent, while in PE/01, which has no detectable FBP expression, an

extra copy of the 22.0-kilobase fragment was apparent. The remaining *Bam*HI fragments in these two lines were present in normal copy. The possible involvement of these rearrangements in FBP expression was not investigated further.

To accompany the studies above, genomic DNA from 10 ovarian carcinomas, one adenoma, one teratoma, and one normal ovary was prepared together with genomic DNA from peripheral blood lymphocytes from the same subjects. These samples were digested with *Pvu*II, and an equal amount of DNA was loaded into each lane of an agarose gel. Southern blot analysis was performed with the cHTMOv18 probe. No amplification was seen in the benign tumors. The FBP locus was amplified by approximately 50% in one of 10 serous adenocarcinomas. All the bands were amplified equally (data not shown). Further studies of these and other samples are underway, but it is clear that overexpression of FBP in ovarian cancer cannot, in general, be due to gene amplification.

DISCUSSION

We describe here the isolation of a cDNA sequence encoding the ovarian cancer-associated antigen recognized by MAb MOv18 and its identification as a high-affinity folate-binding protein. Functional clones were isolated from the ovarian carcinoma cell line SKOV3 and colon carcinoma cell line HT29 using the mammalian expression system first developed by Aruffo and Seed (35). The cDNA thus derived from SKOV3 and HT29 differed in the lengths of 5′- and 3′-noncoding regions but encoded identical peptides of 257 amino acids. A database search clearly showed it to be an adult high-affinity FBP with an amino acid sequence identical with FBPs isolated by different strategies from normal placenta, KB cells (50), and Caco-2 cells (51). MOv18 does not appear to be recognizing an altered form of FBP unique to ovarian cancer since strong reactivity is observed with some normal tissue such as the renal distal and proximal tubules and fallopian tubes (7). Furthermore, the surface expression of the MOv18 antigen among cell lines, as assessed by indirect immunofluorescence, correlated with FBP mRNA levels in all but one case. In this cell line, HT29, it appears that a posttranslational modification results in a form of FBP which is not recognized by MOv18.

In contrast to the percentage of ovarian cancers reported reactive with MOv18, it was demonstrated in only 4 of the 8 ovarian cancer cell lines. At least part of this discrepancy is probably due to down regulation of FBP expression in culture because of the high folate concentration in culture medium (2–20 μM). FBP expression is known to be regulated by internal and external folate levels (54, 55). Increases in FBP expression on the surface of cells grown in folate-deficient medium or at physiological concentrations (5–50 nM) can be 30- to 70-fold higher (55) with subsequent down regulation to "normal" levels when returned to normal culture medium (54). Expression of FBP among the colon carcinoma lines was similar to that of the ovarian lines and might indicate that *in vivo* expression may also be similar. In fact, in studies of 31 colon cancers MOv18 reactivity was seen in only 2 cases (8, 9). The reason for this discrepancy is not understood.

Folic acid plays an essential role in cellular biochemistry, and folate-binding proteins are crucial to the assimilation, distribution, and retention of this vitamin. Two classes of FBPs have been observed in a variety of normal and neoplastic tissue and body fluids (for reviews, see Refs. 56 and 57). High-affinity FBPs constitute the major class and are characterized by their affinities for folate in the nM range. They consist of a water-soluble form found in milk, umbilical cord serum, and at low levels in normal human serum and a membrane form found predominantly on the plasma membranes of tissues from placenta (49), kidney tubules (58), lactating mammary epithelium (56), and in some cultured cell lines (59–61). The membrane form of FBP mediates the transport of folates across plasma membranes via an endocytotic mechanism (62) and *in vitro* enables cells to proliferate in medium containing low folate concentrations (54, 55, 61, 63). The soluble form of FBP in milk probably serves to concentrate folates in milk and protect them from oxidation during ingestion by the infant. The presence of unsaturated FBP in the small intestine of milk-fed neonates has the additional effect of depriving intestinal flora of their source of folate (64). Serum folate-binding proteins have no clear function but are affected *in vivo* by both folate concentration and hormone levels (56).

A precursor-product relationship exists between the two forms of FBP (51). The membrane form is anchored to the cell membrane via a GPI linkage (51, 65), a fact recently confirmed for CaMOv18 (66), and soluble FBP that is generated from membrane FBP by cleavage of this GPI link, as is the case for alkaline phosphatase (67). The attachment of FBP by a GPI link may be to facilitate the transport of folate via a novel endocytotic process reported by Rothberg *et al.* (62). Alternatively, the sensitivity of GPI links to specific phospholipases, particularly phospholipase D, which are abundant in plasma (68), may provide a means of controlling the expression of FBP at the surface of cells.

A second class of FBPs with affinities for folate in the μM range are present only on cell membranes and function in transport of folates across the cell membrane and are structurally unrelated to the high-affinity FBPs.

The role of high-affinity FBPs in ovarian cancer is intriguing. It is possible that the attachment of FBP by a GPI link may act not only as a means of controlling cell surface expression but may also be involved in cell activation or communication. Simultaneous with protein release by specific phospholipases would be the production of biologically active lipids such as 1,2-diacylglycerol and phosphatidic acid that could cross the plasma membrane and affect intracellular metabolism (67). A number of lymphocyte proteins that use GPI anchors have been shown to be capable of mediating mitogenic responses and have been implicated as a second messenger of insulin action (69). Another possibility is that folate levels in the ovary and the uterus are limiting and increased membrane FBP confers a metabolic advantage to cancer cells since they can sequester more folate from serum. Alternatively, its involvement in ovarian cancer may be purely nutritional, reflecting the increased folate requirement of rapidly growing cells.

If any of the above explanations are true, then it would be reasonable to expect overexpression of FBP to be a general phenomenon among many different cancers. In fact, the studies so far reported in the literature show that significantly elevated FBP levels predominate among ovarian carcinomas and to a lesser extent cervical cancers. What special conditions exist in these tissues that selectively elevate FBP expression or limit the bioavailability of folates? There is mounting evidence that hormonal levels affect FBP and folate levels. In the rat uterus cyclic variations in folate coenzymes normally occur during successive stages of the reproductive cycle (70, 71) and increased levels of serum FBPs and folic acid have been observed during pregnancy (72) and with oral contraceptive use (73). Also in

breast cancer serum FBP levels are lower in estrogen receptor-positive cancers and higher in estrogen receptor-negative ones (74). A report by Butterworth *et al.* (75) demonstrated the beneficial effect of folate supplementation in cervical dysplasia in women receiving oral contraceptives. Although there was no evidence of systemic folate deficiency, oral folate supplementation resulted in restoration of a normal epithelium in a significant number of cases and led the authors to propose that chronic exposure of the cervix to contraceptive steroids might produce localized deficiencies in folic acid metabolism that may favor neoplastic transformation.

The mechanism by which FBP expression is elevated in vitro and *in vivo* does not, in general, involve gene amplification, although the rearrangements evident in HeLa and PE/01 cell lines may involve regions containing regulatory elements. It is noteworthy that the 5′-noncoding regions of all the FBP cDNA sequences so far reported are different and may have functional significance. Alternative processing of RNA is a mechanism used by eukaryotic cells to generate multiple transcripts from a single gene and allows several possibilities for modulation of gene expression. Untranslated 5′ regions may affect mRNA stability or the translational capacity of the transcript allowing for expression in a tissue-specific manner (76, 77). A control mechanism that may have particular relevance to FBP expression in ovarian cancer is that of the rat insulin-like growth factor in which transcripts containing one of three alternate 5′-untranslated regions are differentially regulated by growth hormone (78).

Although the role of FBP in ovarian cancer is unclear, it nevertheless provides a unique opportunity to target such cells not only by specific MAbs but also by virtue of the high affinity and high specificity of FBP for folates and folate analogues. Indeed, the small molecular size of such analogues compared to MAbs should also be of considerable advantage. Alternative therapies involving antifolate drugs which can utilize or interfere with the activity of high-affinity FBP may be useful in killing ovarian cancer cells which rely solely on these for folate acquisition. One such folate analogue, homofolate, has been used successfully *in vitro* and specifically inhibits the growth of cells utilizing the high-affinity FBPs but not those using other folate transport systems (79).

FBP may also be important in cellular responses to other chemotherapeutic agents such as the first-line treatment cisplatin (80). Studies of the effects of cisplatin on ovarian cancer cell lines (81, 82) suggest that elevated FBP may influence its pharmacological effects and may be an important component in the pathway leading to cisplatin resistance.

The location of the FBP locus on 11q13.3–14.1 places it near INT2, the human homologue of the murine mammary virus integration site (83). Preliminary studies have indicated that in breast cancers that are amplified for INT2 approximately 25% also have a 2-fold amplification of the FBP locus.[3] Other oncogenes and putative tumor suppressor genes have been mapped to this region including the HST1 (heparin-binding secretory transforming factor) gene (84) and PP1 (protein phosphatase) (85). Translocations involving 11q13 and 14q32.3 are frequently observed in several human pathologies and a rare folate-sensitive fragile site is located at 11q13.3 (86). Studies of this important region may benefit from the *Pst*I and *Msp*I polymorphisms in the FBP loci we have identified.

Although many cancer-associated cell surface antigens have been identified by MAbs, most are poorly characterized. The isolation of cDNA clones for the MOv18 antigen represents a significant advance in the understanding of the nature and function of tumor markers and is one of only a few reports of genes for such antigens being cloned (87–89). The information thus provided should assist in elucidating the mechanism(s) of action and resistance to chemotherapeutic agents and also provides insight into devising alternative therapies. Further study of the genomic organization of the FBP genes is warranted in order to identify the factors that regulate FBP gene expression and to assess the possible involvement of alternative transcripts in the elevation of FBP expression in ovarian cancer.

[3] V. Fantl, unpublished results.

ACKNOWLEDGMENTS

We would like to thank Dr. R. Bolhuis for bringing to our attention the importance of MOv18.

REFERENCES

1. Bast, R. C., Jr., Boyer, C. M., Olt, G. J., Berchuck, A., Soper, J. T., Clarke-Pearson, D., Xu, F. J., and Ramakrishnan, S. Identification of markers for early detection of epithelial ovarian cancer. *In:* F. Sharp, W. P. Mason, and R. E. Leake (eds.), Ovarian Cancer Biological and Therapeutic Challenges, pp. 265–275. London, England: Chapman and Hall Medical, 1990.
2. Bast, R. C., Jr., Feeney, M., Lazarus, H., Nadler, L. M., Colvin, R. B., and Knapp, R. C. Reactivity of a monoclonal antibody with human ovarian carcinoma. J. Clin. Invest., *68:* 1331–1337, 1981.
3. Bast, R. C., Jr., Hunter, V., and Knapp, R. C. Pros and cons of gynecological tumor markers. Cancer (Phila.), *60:* 1984–1992, 1987.
4. Hakomori, S. Tumor-associated carbohydrate antigens. Annu. Rev. Immunol., *2:* 103–126, 1984.
5. Girling, A., Bartkova, J., Burchell, J., Gendler, S., Gillett, C., and Taylor-Papadimitriou, J. A core protein epitope of the polymorphic epithelial mucin detected by the monoclonal antibody SM-3 is selectively exposed in a range of primary carcinomas. Int. J. Cancer, *43:* 1072–1076, 1989.
6. Miotti, S., Canevari, S., Menard, S., Mezzanzanica, D., Porro, G., Pupa, S. M., Reganzzoni, M., Tagliabue, E., and Colnaghi, M. I. Characterization of human ovarian carcinoma-associated antigens defined by novel monoclonal antibodies with tumor-restricted specificity. Int. J. Cancer, *39:* 297–303, 1987.
7. Veggian, R., Fasolato, S., Menard, S., Minucci, D., Pizzetti, P., Regazzoni, M., Tagliabue, E., and Colnaghi, M. I. Immunohistochemical reactivity of a monoclonal antibody prepared against human ovarian carcinoma on normal and pathological female genital tissues. Tumori, *75:* 510–513, 1989.
8. Boerman, O. C., van Niekerk, C. C., Makkink, K., Hanselaar, T. G. J. M., Kenemans, P., and Poels, L. G. Comparative immunohistochemical study of four monoclonal antibodies directed against ovarian carcinoma-associated antigens. Int. J. Gynecol. Pathol., *10:* 15–25, 1991.
9. van Niekerk, C. C., Jap, P. H. K., Thomas, C. M. G., Smeets, D. F. C. M., Ramaekers, F. C. S., and Poels, L. G. Marker profile of mesothelial cells *versus* ovarian carcinoma cells. Int. J. Cancer, *43:* 1065–1071, 1989.
10. Mattes, M. J., Major, P. P., Goldenberg, D. M., Dion, A. S., Hutter, R. V. P., and Klein, K. M. Patterns of antigen distribution in human carcinomas. Cancer Res., *50:* 880–884, 1990.
11. Fogh, J., Wright, W. C., and Lovelass, J. D. Absence of HeLa cell contamination in 169 cell lines derived from human tumors. J. Natl. Cancer Inst., *58:* 209–214, 1977.
12. Langdon, S. P., Lawrie, S. S., Hay, F. G., Hawkes, M. M., McDonald, A., Hayward, I. P., Schol, D. J., Hilgers, J., Leonard, R. C. F., and Smyth, J. F. Characterization and properties of nine human ovarian adenocarcinoma cell lines. Cancer Res., *48:* 6166–6172, 1988.
13. Hill, B. T., Whelan, R. D. H., Gibby, E. M., Sheer, D., Hosking, L. K., Shelland, S. A., and Rupniak, T. Establishment and characterization of three new human ovarian carcinoma cell lines and initial evaluation of their potential in experimental chemotherapy studies. Int. J. Cancer, *39:* 219–225, 1987.
14. Leibovitz, A., Stinson, J. C., McCombs, W. B., III, McCoy, C. E., Mazur, K. C., and Mabry, N. D. Classification of human colorectal adenocarcinoma cell lines. Cancer Res., *36:* 4562–4569, 1976.
15. Fogh, M., and Trempe, G. New human tumor cell lines. *In:* J. Fogh (ed.), Human Tumor Cells *in Vitro*, pp. 115–141. New York: Plenum Press, 1975.
16. Tom, B. H., Rutzky, L. P., Jakstys, M. M., Oyasu, R., Kaye, G. I., and Kahan, B. D. Human colorectal adenocarcinoma cells. I. Establishment and description of a new line. In Vitro, *12:* 180–191, 1976.
17. Drewinco, B., Romsdhal, M. M., Yang, L. Y., Ahearn, M. J., and Trujillo, J. M. Establishment of a human CEA producing colon adenocarcinoma cell line. Cancer Res., *36:* 467–475, 1976.
18. Dexter, D. L., Barbosa, J. A., and Calabresi, P. *N,N*-dimethylformamide-induced alteration of cell culture characteristics and loss of tumorgenicity in culture human colon carcinoma cells. Cancer Res., *39:* 1020–1025, 1979.

19. Brattain, M. G., Fine, W. D., Khaled, F. M., Thompson, J., and Brattain, D. E. Heterogeneity of malignant cells from human colonic carcinoma. Cancer Res., *41:* 1751–1756, 1981.
20. Greenhalgh, D. A., and Kinsella, A. R. c-Ha-*ras* not c-Ki-*ras* activation in three tumor cell lines. Carcinogenesis (Lond.), *6:* 1533–1535, 1985.
21. Soule, H. D., Vazquez, J., Long, A., Albert, S., and Brennan, M. A human cell line from a pleural effusion derived from a breast carcinoma. J. Natl. Cancer Inst., *51:* 1409–1416, 1973.
22. Kozbor, D., and Croce, C. M. Amplification of the c-*myc* oncogene in one of five human breast carcinoma cell lines. Cancer Res., *44:* 438–441, 1984.
23. Santos, E., Traonick, S. R., Aaronson, S. A., Pulciani, S., and Barbacid, M. Human EJ bladder carcinoma oncogene is homologue of BALB- and Harvey-MSV transforming gene. Nature (Lond.), *298:* 343–347, 1982.
24. Rasheed, S., Nelson-Rees, W. A., Toth, E. M., Arnstein, P., and Gardner, M. B. Characterization of a newly derived human sarcoma cell line (HT-1080). Cancer (Phila.), *33:* 1027–1033, 1974.
25. Nelson-Rees, W. A., and Flandermeyer, R. R. HeLa cultures defined. Science (Washington DC), *191:* 96–98, 1976.
26. Minowasa, J., Ohnuma, T., and Moore, G. E. Rosette-forming human lymphoid cell lines. I. Establishment and evidence for origin of thymus-derived lymphocytes. J. Natl. Cancer Inst., *49:* 891–895, 1972.
27. Kozlowski, J. M., Fidler, I. J., Campbell, D., Xu, Z., Kaighn, M. E., and Hart, I. R. Metastatic behavior of human tumor cell lines grown in the nude mouse. Cancer Res., *44:* 3522–3529, 1986.
28. Brodsky, F. M., Parham, P., Barnstable, C. J., Crumpton, M. J., and Bodmer, W. F. Monoclonal antibodies for analysis of the HLA system. Immunol. Rev., *47:* 3–61, 1979.
29. Jacobs, J. P., Jones, C. M., and Baille, J. P. Characteristics of a human diploid cell designated MRC-5. Nature (Lond.), *227:* 168–170, 1970.
30. Erikson, J., Ar-Rushdi, A., Drwinga, H. L., Nowell, P. C., and Croce, C. M. Transcriptional activation of the translocated c-*myc* oncogene in Burkitt lymphoma. Proc. Natl. Acad. Sci. USA, *80:* 820–824, 1983.
31. Flugel, R. M., Crefeld, T., and Munk, K. Detection of SV40 antigen with labelled antibodies: radioimmunoassay and autoradiography. Int. J. Cancer, *19:* 656–663, 1977.
32. Seed, B. An LFA-3 cDNA encodes a phospholipid membrane protein homologous to its receptor CD2. Nature (Lond.), *329:* 840–842, 1987.
33. Dailey, L., and Basllico, C. Sequences in the polyomavirus DNA regulatory region involved in viral replication and early gene expression. J. Virol., *54:* 739–749, 1985.
34. Chu, G., Hayakawa, H., and Berg, P. Electroporation for the efficient transfection of mammalian cells with DNA. Nucleic Acids Res., *15:* 1311–1326, 1987.
35. Aruffo, A., and Seed, B. Molecular cloning of a CD28 cDNA by a high-efficiency COS cell expression system. Proc. Natl. Acad. Sci. USA, *84:* 8573–8577, 1987.
36. Birnboim, H. C., and Doly, J. A rapid alkaline extraction procedure for screening recombinant plasmid DNA. Nucleic Acids Res., *7:* 1513–1523, 1979.
37. Maniatis, T., Fritsch, E. F., and Sambrook, J. Molecular Cloning: A Laboratory Manual. Cold Spring, NY: Cold Spring Harbor Laboratory, 1982.
38. Croce, C. M., and Koprowski, H. Somatic cell hybrids between mouse peritoneal macrophages and SV-40 transformed human cells. J. Exp. Med., *140:* 1221–1229, 1974.
39. Solomon, E., Bobrow, M., Goodfellow, P. N., Bodmer, W. F., Swallow, D. M., Povey, S., and Noel, B. Human gene mapping using an X/autosome translocation. Somat. Cell Genet., *2:* 125–140, 1976.
40. Edwards, Y. H., Parkar, M., Povey, S., West, L. F., Parrington, F. M., and Solomon, E. Human myosin heavy chain genes assigned to chromosome 17 using a human cDNA clone as probe. Ann. Hum. Genet., *49:* 101–109, 1985.
41. Jones, E. A., Goodfellow, P. N., Kennett, R. H., and Bodmer, W. F. The independent expression of HLA and β2 microglobulin on human-mouse hybrids. Somat. Cell Genet., *2:* 483–496, 1976.
42. Hobart, M. J., Rabbitts, T. H., Goodfellow, P. N., Solomon, E., Chambers, S., Spurr, N., and Povey, S. Immunoglobulin heavy chain genes map to chromosome 14. Ann. Hum. Genet., *45:* 331–335, 1981.
43. Jones, C., Bill, J., Larizza, L., Bym, G., Geedfellow, P., and Tunnacliffe, A. Relationship between genes on human chromosome 11, encoding cell surface antigens. Somat. Cell Mol. Genet., *10:* 423–428, 1984.
44. Edwards, Y., West, L., Van Heyningen, V., Cowell, J., and Goldberg, E. Regional localization of the sperm-specific lactate dehydrogenase, LDHC, gene on human chromosome 11. Ann. Hum. Genet., *53:* 215–219, 1989.
45. Chiang, Y. L., Ley, T. J., Sanders-Haigh, L., and Anderson, W. F. Human globin gene expression in hybrid 2S MEL × human fibroblast cells. Somat. Cell Mol. Genet., *10:* 399–407, 1984.
46. Pinkel, D., Landegent, J., Collins, C., Fuscoe, J., Segraves, R., Lucas, J., and Gray, J. Fluorescence *in situ* hybridization with human chromosome-specific libraries: detection of trisomy 21 and translocations of chromosome 4. Proc. Natl. Acad. Sci. USA, *85:* 9138–9142, 1985.
47. Lichter, P., Tang, C., Call, K., Hermanson, G., Evans, G. A., Housman, D., and Ward, D. C. High-resolution mapping of human chromosome 11 by *in situ* hybridization with cosmid clones. Science (Washington DC), *247:* 264–268, 1989.
48. Harnden, D. G., and Klinger, H. P. An International System for Human Cytogenetic Nomenclature. Basel, Switzerland: Karger, 1985.
49. Ratnam, M., Marquardt, H., Duhring, J. L., and Freisheim, J. H. Homologous membrane folate binding proteins in human placenta: cloning and sequence of a cDNA. Biochemistry, *28:* 8249–8254, 1989.
50. Elwood, P. C. Molecular cloning and characterization of the human folate-binding protein cDNA from placenta and malignant tissue culture (KB) cells. J. Biol. Chem., *264:* 14893–14901, 1989.
51. Lacey, S. W., Sanders, J. M., Rothberg, K. G., Anderson, R. G. W., and Kamen, B. A. Complementary DNA for the folate binding protein correctly predicts anchoring to the membrane by glycosyl-phosphatidylinositol. J. Clin. Invest., *84:* 715–720, 1990.
52. Sadasivan, E., and Rothenberg, S. P. The complete amino acid sequence of a human folate binding protein from KB cells determined from the cDNA. J. Biol. Chem., *264:* 5806–5811, 1989.
53. Waye, J. S., Greig, G. M., and Willard, W. F. Detection of novel centromeric polymorphisms associated with alpha satellite DNA from human chromosome 11. Hum. Genet., *77:* 151–156, 1987.
54. Kamen, B. A., and Capdevila, A. Receptor-mediated folate accumulation is regulated by cellular folate content. Proc. Natl. Acad. Sci. USA, *83:* 5983–5987, 1986.
55. Jansen, G., Kathmann, I., Rademaker, B. C., Braakhuis, B. J. M., Westerhof, G. R., Rijksen, G., and Schornagel, J. H. Expression of a folate binding protein in L1210 cells grown in low folate medium. Cancer Res., *49:* 1959–1963, 1989.
56. Henderson, G. B. Folate binding proteins. Annu. Rev. Nutr., *10:* 319–335, 1990.
57. Kane, M. A., and Waxman, S. Biology of disease: role of folate binding proteins in folate metabolism. Lab. Invest., *60:* 737–746, 1989.
58. Selhub, J., Nakamura, S., and Carone, F. A. Renal folate absorption and the kidney folate binding protein. II. Microinfusion studies. Am. J. Physiol., *252:* F757–F760, 1987.
59. McHugh, M., and Cheng, Y. C. Demonstration of a high-affinity folate binder in human cell membranes and its characterization in human KB cells. J. Biol. Chem., *254:* 11312–11318, 1979.
60. Jansen, G., Westerhof, G. R., Kathmann, I., Rademaker, B. C., Rijksen, G., and Schornagel, J. H. Identification of a membrane-associated folate-binding protein in human leukemic CCRF-CEM cells with transport-related methotrexate. Cancer Res., *49:* 2455–2459, 1989.
61. Henderson, G. B., Tsuji, J. M., and Kumar, H. P. Mediated uptake of folate by a high affinity binding protein in sub-lines of L1210 cells adapted to nanomolar concentrations of folate. J. Membr. Biol., *101:* 247–258, 1988.
62. Rothberg, K. G., Ying, Y., Kolhouse, J. F., Kamen, B. A., and Anderson, R. G. W. The glycophospholipid-linked folate receptor internalizes folate without entering the clathrin-coated pit endocytic pathway. J. Cell Biol., *110:* 637–649, 1990.
63. Kane, M. A., Elwood, P. C., Portillo, R. M., Antony, A. C., Najfeld, V., Finley, A., Waxman, S., and Kolhouse, J. F. Influence on immunoreactive folate binding proteins of extracellular folate concentration in cultured human cells. J. Clin. Invest., *81:* 1398–1406, 1988.
64. Ford, J. E. Some observations on the possible nutritional significance of vitamin B12 and folate binding proteins in milk. Br. J. Nutr., *31:* 335–342, 1974.
65. Luhrs, C. A., and Slomiany, B. L. A human membrane-associated folate binding protein is anchored by a glycosyl-phosphatidylinositol tail. J. Biol. Chem., *264:* 21446–21449, 1989.
66. Alberti, S., Miotti, S., Fornaro, M., Mantovani, L., Walter, S., Canevari, S., Menard, S., and Colnaghi, M. I. The Ca-MOv18 molecule, a cell-surface marker of human ovarian carcinomas, is anchored to the cell membrane by phosphatidylinositol. Biochem. Biophys. Res. Commun., *171:* 1051–1055, 1990.
67. Low, M. G., and Saltiel, A. R. Structural and functional roles of glycosyl-phosphatidylinositol in membranes. Science (Washington DC), *239:* 268–275, 1988.
68. Low, M. G., and Prasad, A. R. S. A phospholipase D specific for the phosphatidylinositol anchor of cell-surface proteins is abundant in plasma. Proc. Natl. Acad. Sci. USA, *85:* 980–984, 1988.
69. Low, M. G. Glycosyl-phosphatidylinositol: a versatile anchor for cell surface proteins. FASEB J., *3:* 1600–1608, 1990.
70. Krumdieck, C. L., Boots, L. R., Cornwell, P. E., and Butterworth, C. E., Jr. Estrogen stimulation of conjugase activity in the uterus of ovariectomized rats. Am. J. Clin. Nutr., *28:* 530–534, 1976.
71. Krumdieck, C. L., Boots, L. R., Cornwell, P. E., and Butterworth, C. E., Jr. Cyclic variations in folate composition and pteroylpolyglutamyl hydrolase (conjugase) activity of the rat uterus. Am. J. Clin. Nutr., *29:* 288–294, 1976.
72. Holm, J., Hansen, S. I., and Lyngbye, J. High and low affinity binding of folate to proteins in serum of pregnant women. Biochim. Biophys. Acta, *629:* 539, 1980.
73. Joshi, U. M., Virkar, K. D., Amatayakul, K., Singkamani, R., Bamji, M. S., Prema, K., Whitehead, T. P., Belsey, M. A., Hall, P., Parker, R. A., *et al.* Impact of hormonal contraceptives vis-a-vis non-hormonal factors on the vitamin status of malnourished women in India and Thailand. Hum. Nutr. Clin. Nutr., *40:* 205–220, 1986.
74. Rochman, H., Selhub, J., and Karrison, T. Folate binding protein and estrogen receptor in breast cancer. Cancer Detect. Prev., *8:* 71, 1985.
75. Butterworth, C. E., Jr., Hatch, K. D., Gore, H., Mueller, H., and Krumdieck, C. L. Improvement in cervical dysplasia associated with folic acid therapy in users of oral contraceptives. Am. J. Clin. Nutr., *35:* 73–82, 1982.
76. Leff, S. E., and Rosenfeld, M. G. Complex transcriptional units: diversity in gene expression by alternative RNA processing. Annu. Rev. Biochem., *55:* 1091–1117, 1986.

77. Chobert, M. N., Lahuna, O., Lebargy, F., Kurauchi, O., Darbouy, M., Bernaudin, J. F., Guellaen, G., Barouki, R., and Laperche, Y. Tissue specific expression of two γ-glutamyl transpeptidase mRNAs with alternative 5′ ends encoded by a single copy gene in the rat. J. Biol. Chem., *265:* 2352–2357, 1990.
78. Low, W. L., Jr., Roberts, C. T., Jr., Lasky, S. R., and LeRoith, D. Differential expression of alternative 5′ untranslated regions in mRNAs encoding rat insulin-like growth factor. Proc. Natl. Acad. Sci. USA, *84:* 8946–8950, 1987.
79. Henderson, G. B., and Strauss, B. P. Growth inhibition by homofolate in tumor cells utilizing a high-affinity folate binding protein as a means for folate internalization. Biochem. Pharmacol., *39:* 2019–2025, 1990.
80. Lund, B., and Hansen, H. H. Chemotherapy in ovarian cancer. Cancer Surv., *8:* 681–691, 1990.
81. Scanlon, K. J., Newman, E. M., Lu, Y., and Priest, D. G. Biochemical basis for cisplatin and 5-fluorouracil synergism in human ovarian carcinoma cells. Proc. Natl. Acad. Sci. USA, *83:* 8923–8925, 1986.
82. Lu, Y., Han, J., and Scanlon, K. J. Biochemical and molecular properties of cisplatin-resistant A2780 cells grown in folinic acid. J. Biol. Chem., *263:* 4891–4894, 1988.
83. Casey, G., Smith, R., McGillvray, D., Peters, G., and Dickson, C. Characterization and chromosome assignment of the homolog of *int*-2, a potential proto-oncogene. Mol. Cell Biol., *6:* 502–510, 1986.
84. Yoshida, M. C., Wada, M., Satoh, H., Yoshida, T., Sakamoto, H., Miyagawa, K., Yokota, J., Koda, T., Kakinuma, M., Sugimura, T., and Terada, M. Human HST1 (HSTF1) gene maps to chromosome band 11q and co-amplifies with the INT2 gene in human cancer. Proc. Natl. Acad. Sci. USA, *85:* 4861–4864, 1988.
85. Barker, H. M., Jones, T. A., Da Cruze Silva, E. F., Spurr, N. K., Sheer, D., and Cohen, P. T. W. Localization of the gene encoding a type I protein phosphatase catalytic subunit to human chromosome band 11q13. Genomics, *7:* 159–166, 1990.
86. Julier, C., Nakamura, Y., Lathrop, M., O'Connell, P., Leppert, M., Litt, M., Mohandas, T., Lalouel, J., and White, R. A detailed genetic map of the long arm of chromosome 11. Genomics, *7:* 335–345, 1990.
87. Zimmermann, W., Ortlieb, B., Friedrich, R., and von Kleist, S. Isolation and characterization of cDNA clones encoding the human carcinoembryonic antigen reveal a highly conserved repeating structure. Proc. Natl. Acad. Sci. USA, *84:* 2960–2964, 1987.
88. Hotta, H., Ross, A. H., Huebner, K., Isobe, M., Wendeborn, S., Chao, M. V., Ricciardi, R. P., Tsujimoto, Y., Croce, C. M., and Koprowski, H. Molecular cloning and characterization of an antigen associated with early stages of melanoma tumor progression. Cancer Res., *48:* 2955–2962, 1988.
89. Strnad, J., Hamilton, A. E., Beavers, L. S., Gamboa, G. C., Apelgren, L. D., Taber, L. D., Sportsman, J. R., Bumol, T. F., Sharp, J. D., and Gadski, R. A. Molecular cloning and characterization of a human adenocarcinoma/epithelial cell surface antigen complementary DNA. Cancer Res., *49:* 314–317, 1989.